

Final-state interactions in the $^{12}\text{C}(^{16}\text{O}, ^{12}\text{C}^{12}\text{C})\alpha$ and $^{16}\text{O}(^{16}\text{O}, ^{12}\text{C}^{16}\text{O})\alpha$ reactions

M. Freer, N. M. Clarke, R. A. Le Marechal, G. Tungate, and R. P. Ward

School of Physics and Space Research, University of Birmingham, Birmingham, B15 2TT, United Kingdom

W. D. M. Rae

Department of Physics, University of Oxford, Nuclear Physics Laboratory, Keble Road, Oxford, OX1 3RH, United Kingdom

(Received 9 January 1995)

The population of excited states in ^{24}Mg and ^{28}Si has been investigated through the reactions $^{12}\text{C}(^{16}\text{O}, ^{12}\text{C}^{12}\text{C})\alpha$ and $^{16}\text{O}(^{16}\text{O}, ^{12}\text{C}^{16}\text{O})\alpha$, at beam energies of 80.5 and 99 MeV. The heavy-ion fragments from the breakup of the ^{24}Mg and ^{28}Si nuclei were detected in coincidence, permitting a study of both the reaction kinematics and the spins of the fissioning states. These measurements indicate a series of states in ^{24}Mg between 25 and 32 MeV with spins ranging from $J=10$ to $14\hbar$. Evidence was also found for the breakup of ^{28}Si into $^{12}\text{C}+^{16}\text{O}$ from states between 27 and 29 MeV.

PACS number(s): 25.70.Ef, 27.30.+t

I. INTRODUCTION

The appearance of resonances in many scattering systems has motivated a considerable number of experiments [1]. However, it is the study of the resonance phenomena in ^{24}Mg which has attracted the most attention. Detailed measurements of the energies, spins, and partial decay widths of resonances observed in this system, using a variety of experimental techniques, have identified groups of resonances with common structural properties.

More recently, studies of breakup reactions have observed highly excited states in ^{24}Mg which fission into two ^{12}C nuclei, e.g., $^{12}\text{C}(^{24}\text{Mg}, ^{12}\text{C}^{12}\text{C})^{12}\text{C}$ [2,3]. This experimental technique differs from the earlier studies of resonances in colliding systems, in that the spectrum of states populated in the ^{24}Mg nucleus is not constrained to a particular energy or angular momentum. Typically, a spectrum of excitation energies with a range of angular momenta may be accessed in a single measurement. The drawback of such reactions is that they result in the production of three or more particles in the final state. This has necessitated the development of multiple particle coincidence detection techniques in order to reconstruct fully the reaction kinematics and to extract spin assignments from an analysis of the breakup angular correlations.

A number of studies of the $^{12}\text{C}(^{16}\text{O}, \alpha)^{24}\text{Mg}^*$ reaction have been performed [4–7], which appeared to indicate the formation of a number of highly excited states in ^{24}Mg . These states were thought to correspond to the resonances in $^{12}\text{C}+^{12}\text{C}$ inelastic scattering measurements first observed by Cormier *et al.* [8,5]. However, the detection of the α particles alone does not constrain the reaction sufficiently, as there is a large α -particle contribution from the $^{12}\text{C}(^{16}\text{O}, ^{12}\text{C}, \alpha)^{12}\text{C}$ projectile breakup reaction. In fact, it has been demonstrated that the majority of the structures in the α -particle singles spectra could be attributed to projectile breakup [9–13]. Detailed measurements of the kinematic behavior of the peaks in the α -particle spectra [14,15] did, however, indicate that

some of the smaller structures could be associated with the formation of ^{24}Mg excited states.

Coincident experiments, where a ^{12}C nucleus is detected along with the α -particle recoil [16] or where two ^{12}C nuclei were detected [17], found further evidence for a series of states between 25–35 MeV with large $^{12}\text{C}+^{12}\text{C}$ decay widths [16]. The first measurements of the spins of the ^{24}Mg states populated through this reaction were made by Costanzo *et al.* [18–20]. In these measurements, the coincidence detection of the two ^{12}C nuclei with position sensitive detectors permitted a complete reconstruction of the $^{12}\text{C}+^{12}\text{C}+\alpha$ final state, facilitating the elimination of the contribution from projectile breakup. This detection technique also allowed the angular correlations of the final state particles to be studied, and thus the spins of the ^{24}Mg states to be deduced. A number of states between 25 and 37 MeV were identified, and a spin of $J = 12\hbar$ was inferred for states at 30.7 and 31.6 MeV and $J = 14\hbar$ for states at 35.1 and 36.5 MeV. On the basis of these measurements the authors suggested a connection between these ^{24}Mg states and resonances observed in the $^{12}\text{C}(^{12}\text{C}, \alpha)$ and $^{12}\text{C}(^{12}\text{C}, ^8\text{Be})$ reactions [1,21,22]. These “barrier resonances” are believed to be evidence of the rotational and vibrational degrees of freedom of a quasimolecular $^{12}\text{C}+^{12}\text{C}$ configuration [23].

In general, the existing data are rather limited, and thus it is important to establish the full energy-spin systematics of the ^{24}Mg states populated in the $^{12}\text{C}(^{16}\text{O}, ^{12}\text{C}^{12}\text{C})\alpha$ reaction in order to confirm the connection with a quasimolecular $^{12}\text{C}+^{12}\text{C}$ configuration. In this paper we report further measurements of the spins of ^{24}Mg states populated in the $^{12}\text{C}(^{16}\text{O}, ^{12}\text{C}^{12}\text{C})\alpha$ reaction at $E_{\text{beam}}=80.5$ MeV and 99 MeV. We also report on the search for the formation of ^{28}Si excited states through the $^{16}\text{O}(^{16}\text{O}, ^{16}\text{O}^{12}\text{C})\alpha$ reaction at the same beam energies.

II. EXPERIMENTAL DETAILS

The $^{12}\text{C}(^{16}\text{O}, ^{12}\text{C}^{12}\text{C})\alpha$ and $^{16}\text{O}(^{16}\text{O}, ^{12}\text{C}^{16}\text{O})\alpha$ reactions have been studied with beam energies of 80.5 MeV

and 99 MeV, produced from the Australian National University's 14UD tandem accelerator. The integrated beam exposures were 11 mC and 4 mC for the beam energies 80.5 and 99 MeV, respectively.

The target foils employed in these measurements were composed of $200 \mu\text{g cm}^{-2}$ of B_2O_3 on a backing of $10 \mu\text{g cm}^{-2}$ of ^{12}C . This particular target allowed the simultaneous study of a number of different reactions. The reaction parameters determined by the detection system used in these measurements permitted the identification and separation of the products from the various target components.

The two heavy ions produced in these reactions were detected in two gas-silicon hybrid detectors [24]. The silicon elements of these detectors were $5 \times 5 \text{ cm}^2$ 16 strip, position sensitive silicon strip detectors (PSSSD's). The strips were orientated horizontally such that the detectors determined the position of the incident nuclei to within $200 \mu\text{m}$ in this direction, whereas the measurement of the vertical position was determined by the strip pitch ($3000 \mu\text{m}$). The gas detectors were operated at a pressure of 40 Torr of propane, and with $3.5 \mu\text{m}$ Mylar windows. This relatively low propane pressure was used in order that the energy threshold (due to the ΔE - E coincidence requirement) on the detection of the ^{12}C and ^{16}O nuclei was minimized. This permitted the detection of nuclei with energies as small as 15 MeV, while still retaining sufficient Z resolution to perform particle identification.

The hybrid detectors provided a determination of the charge, energy, and emission angle for each of the detected particles. From this information, the momenta of the two detected nuclei were deduced, and through the principle of momentum conservation the momentum of the third, undetected nucleus was determined. The two detectors were positioned symmetrically about the beam axis, and covered the angular ranges 22.25° to 37.75° and 15.25° to 30.75° for the beam energies of 80.5 and 99 MeV, respectively. The energy and position response of the silicon detectors were calibrated with 35 MeV and 45 MeV ^{12}C ions and 39 MeV ^{16}O ions scattered from ^{12}C , ^{27}Al , and ^{197}Au targets.

III. RESULTS AND DATA ANALYSIS

A. The $^{12}\text{C}(^{16}\text{O}, ^{12}\text{C}^{12}\text{C})\alpha$ reaction

Figure 1 shows the three-body Q -value (Q_3) spectrum for events in which two ^{12}C nuclei were detected, and for an assumed α -particle recoil. In this instance the beam energy was 80.5 MeV. The reaction Q value can be deduced from the following relationship

$$Q_3 = E_{\text{beam}} - E_{^{12}\text{C}(1)} - E_{^{12}\text{C}(2)} - E_{\alpha}. \quad (1)$$

The energy, E_{α} , of the unobserved α particle was deduced from the momenta of the two detected ^{12}C nuclei. The peaks in this spectrum correspond to the three possible combinations of the two ^{12}C nuclei being produced in their ground and first excited states ($E_x = 4.4 \text{ MeV}$). The

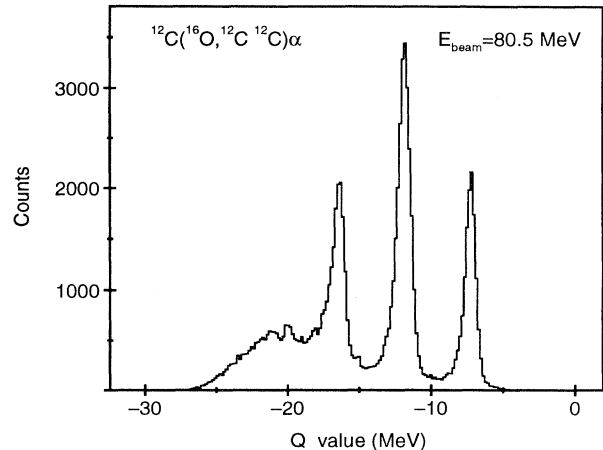


FIG. 1. Three-body Q -value spectrum constructed for the detection of two ^{12}C nuclei and an assumed α recoil.

Q -value energy resolution is $\sim 850 \text{ keV}$ and is dominated by the energy resolution of the hybrid detectors.

The mass of the recoil-like particle was deduced from a comparison of the calculated recoil momentum with the recoil energy using the technique developed by Costanzo *et al.* [19]. The mass of the unobserved particle can be deduced from the gradient of the Q_3 loci in a plot of $E_{\text{beam}} - E_{^{12}\text{C}(1)} - E_{^{12}\text{C}(2)}$ against the recoil momentum, which is deduced from the momenta of the two ^{12}C nuclei. This analysis confirmed the inferred recoil mass of $A = 4$, and furthermore that there was no evidence for any contribution from the reaction $^{10}\text{B}(^{16}\text{O}, ^{12}\text{C}^{12}\text{C})^2\text{H}$ ($Q_3 = -5.83 \text{ MeV}$).

The relative kinetic energies (E_{rel}) of the three final state particles were calculated for the case that both ^{12}C nuclei were in the ground state

$$E_{\text{rel}} = \frac{1}{2} \frac{m_1 m_2}{m_1 + m_2} v_{\text{rel}(1-2)}^2, \quad (2)$$

where m_1 and m_2 are the masses of the two nuclei and $v_{\text{rel}(1-2)}$ is their relative velocity. The relative energy spectra may be used to indicate which two of the three final state particles were produced from the decay of an excited nucleus. For example, peaks in the reconstructed ^{12}C - α relative energy spectra would indicate that these particles were produced from the decay of an ^{16}O nucleus, or a peak in the ^{12}C - ^{12}C relative energy spectrum would indicate the decay from an excited ^{24}Mg nucleus.

The excitation energy of the ^{16}O nuclei can also be calculated, but with slightly better resolution, through the application of two-body kinematics by assuming each of the two detected ^{12}C nuclei to be the recoil from the reaction $^{12}\text{C}(^{16}\text{O}, ^{16}\text{O}^*)^{12}\text{C}$. The excitation energies of the ^{16}O nuclei calculated in this latter manner are plotted against each other in Fig. 2, again for the 80.5 MeV measurement. It is clear that the dominant contribution to these data is indeed from the decay of excited states in ^{16}O into $^{12}\text{C} + \alpha$, which appear as horizontal and vertical loci in the figure. However, there is also evidence for a series of diagonal trajectories in the excitation energy re-

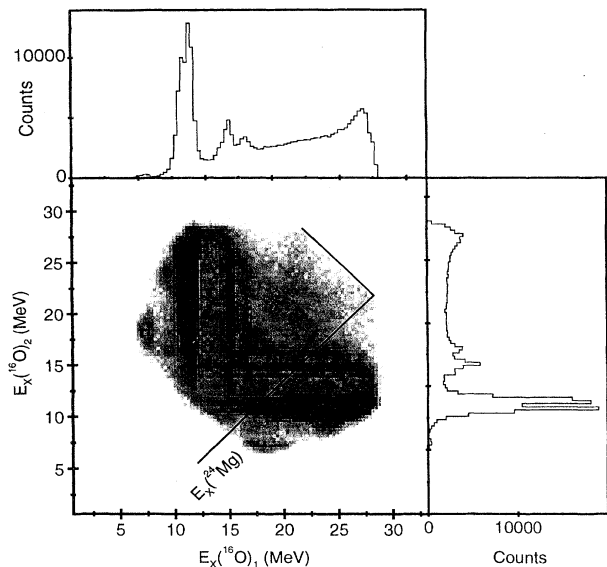


FIG. 2. Plot of the two reconstructed ^{16}O excitation energies. The horizontal and vertical loci correspond to ^{16}O excited states. Evidence for a ^{12}C - ^{12}C final-state interaction may be observed in the region $E_x(^{16}\text{O})_1 > 15$ MeV and $E_x(^{16}\text{O})_2 > 15$ MeV.

gion $E_x(^{16}\text{O})_1 > 15$ MeV and $E_x(^{16}\text{O})_2 > 15$ MeV, which would indicate the presence of a $^{12}\text{C}+^{12}\text{C}$ final-state interaction (FSI).

In order to enhance the relative intensity of the $^{12}\text{C}+^{12}\text{C}$ FSI, the $^{12}\text{C}+\alpha$ data have been excluded below $E_x(^{16}\text{O}) = 16.5$ MeV, a procedure which was also performed by Costanzo *et al.* [18]. Figure 3(a) shows the resulting ^{24}Mg excitation energy spectrum for the 80.5 MeV measurement. There appear to be a number of states with excitation energies of 25.4, 26.2, 27.2, 27.9, 29.0, and 31.5 MeV and there is an indication of further states at 23.0, 29.7, and 32.6 MeV. These excitation energies should be compared with those reported by Costanzo *et al.* [18,19] for the $^{12}\text{C}(^{16}\text{O},^{12}\text{C}^{12}\text{C})\alpha$ reaction studied at 85 MeV. These authors found evidence for a series of states in ^{24}Mg at excitation energies of 26.3, 27.3, 28.4, 29.2, 30.7, and 31.6 MeV. There appears to be good agreement between the data in the spectrum in Fig. 3(a) and the data of Costanzo *et al.*, if the spectra in Fig. 3 are shifted by -700 keV. Such an energy shift would correspond to a 1.5° shift in one of the detector angles in either of the measurements. We have performed a detailed analysis of our data, in particular the ^{16}O excitation energy spectra calculated from the kinematics of the ^{12}C recoil. These spectra are very sensitive to the angles of the detectors. With the calibrated energies and angles, ^{16}O excited states are found at energies of 10.4, 11.1, and 14.8 MeV in good agreement with the tabulated values [25]. Such an agreement cannot be sustained if the angles of the detectors are offset so as to reproduce the ^{24}Mg excitation energies reported in Refs. [18,19]. This analysis would further indicate that the uncertainty in our energy assignments is ± 100 keV.

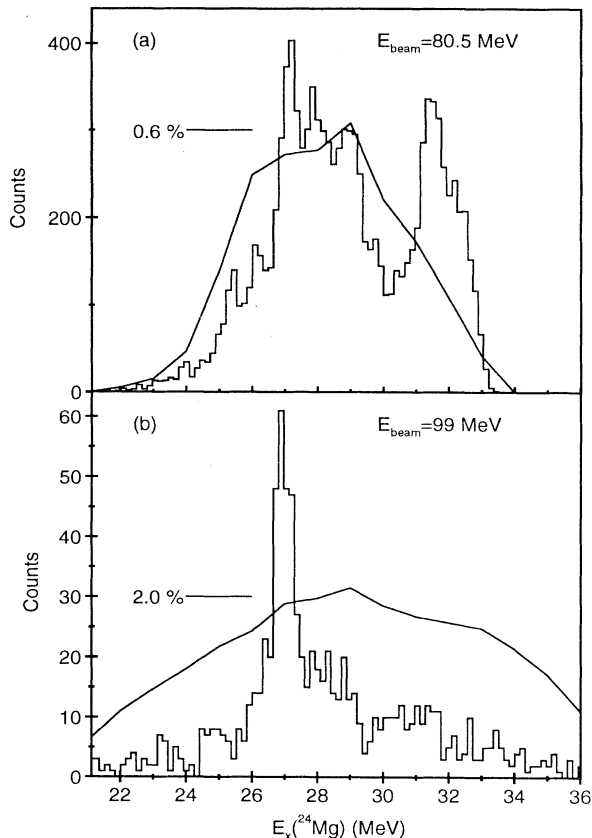


FIG. 3. ^{24}Mg excitation energy spectra overlaid with the calculated detection efficiency. (a) $E_{\text{beam}}=80.5$ MeV, (b) $E_{\text{beam}}=99$ MeV.

Figure 3(a) also shows the detection efficiency determined as a function of the ^{24}Mg excitation energy, using the Monte Carlo technique. This Monte Carlo calculation simulates the response of the detection system, e.g., the energy and angular acceptances, and also the energy and angular distributions of the reaction products. For these calculations, the primary $^{24}\text{Mg}^*-\alpha$ and subsequent decay angular distributions were both assumed to possess a $1/\sin\theta$ dependence. The efficiency profile shown in Fig. 3(a) has also included the effects of the ^{16}O excitation energy restrictions, which were imposed in the data analysis. The efficiency profile indicates that the peak at $E_x(^{24}\text{Mg})=31.5$ MeV is in fact stronger by a factor of 2 than the states between 26–30 MeV and that the states below 26 MeV are similarly suppressed by the reduced detection efficiency.

Figure 4 shows the relative energies of the two ^{12}C nuclei and the α particle for the 99 MeV reaction data. In this instance the detector geometry favored the detection of the ^{12}C - ^{12}C FSI, causing the data to be concentrated on a diagonal line in this figure. The data are shown projected onto the ^{12}C - ^{12}C relative energy axis in Fig. 3(b), which shows that the bulk of the data are restricted to the state at 27.2 MeV. The appearance of a single state in this spectrum may not be attributed to the detection

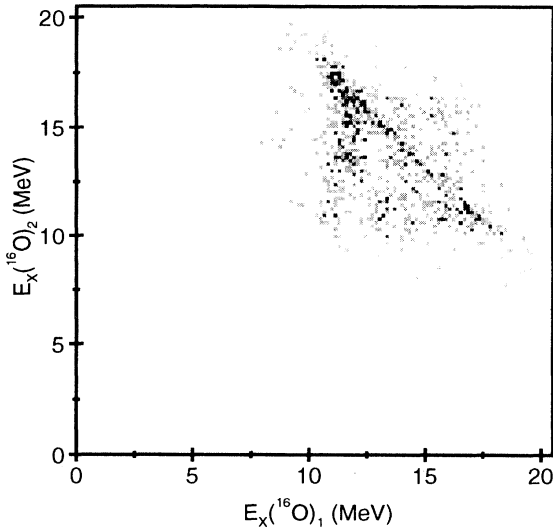


FIG. 4. Plot of the two reconstructed ^{16}O excitation energies for $E_{\text{beam}}=99$ MeV. The ^{12}C - ^{12}C final-state interaction is apparent as a diagonal line.

efficiency, since the Monte Carlo calculations show that experimental arrangement was sensitive to a broad distribution of excitation energies. A comparison of the yields, normalized for detection efficiency, at the two beam energies indicates that there is a reduction in the reaction cross section at the higher beam energy by a factor of 5 for the 27.2 MeV state, and >15 for the other states.

Figures 5(a) and 5(b) show plots of the ^{16}O excitation energies, for the 80.5 MeV data, for the case when one or two of the ^{12}C nuclei are produced in the first excited state [$E_x(^{12}\text{C})=4.4$ MeV, $J^\pi = 2^+$]. Figure 5(a) has been constructed assuming the excited ^{12}C nucleus is the recoil. For the ^{16}O excited states at ~ 15 MeV there is an ambiguity, since these states can also α decay to the ^{12}C , 2^+ state with the recoil particle then in the ground state. This ambiguity results in a fraction of the yield for the 14.8 MeV state being displaced by -4.4 MeV. Again in the energy region $E_x(^{16}\text{O})_1 > 15$ MeV and $E_x(^{16}\text{O})_2 > 15$ MeV, there appears to be evidence for diagonal structure in Fig. 5(a). However, such strong features are not found in Fig. 5(b). Figures 6(a) and 6(b) show the ^{24}Mg excitation energy spectra corresponding to the $^{12}\text{C}(2^+) + ^{12}\text{C}_{\text{gs}}$ and $^{12}\text{C}(2^+) + ^{12}\text{C}(2^+)$ decay channels, produced under the excitation energy constraints $E_x(^{16}\text{O}) > 16.5$ MeV. These spectra do not possess the same degree of structure which was present in the decay to $^{12}\text{C}_{\text{gs}} + ^{12}\text{C}_{\text{gs}}$. However, there is some evidence for two states in the $^{12}\text{C}(2^+) + ^{12}\text{C}_{\text{gs}}$ decay channel at 29.9 and 31.0 MeV, and a state at 31.8 MeV in the $^{12}\text{C}(2^+) + ^{12}\text{C}(2^+)$ channel. These states would appear to have no counterparts in the $^{12}\text{C}_{\text{gs}} + ^{12}\text{C}_{\text{gs}}$ decay channel.

B. Angular correlation measurements

The complete determination of the kinematics of the reaction resulting in the $^{12}\text{C} + ^{12}\text{C} + \alpha$ final state permits

the study of the angular correlations of these particles. The angular correlations may be used to further determine the angular momenta involved in the reaction process, and are described in terms of the two angles θ^* and ψ [26], for correlations confined to the reaction plane. θ^* describes the center of mass emission angle of the excited ^{24}Mg nucleus, and ψ the subsequent emission angle of the ^{12}C fragments, both measured with respect to the beam axis. The correlation angles are illustrated in Fig. 7.

Figure 8 shows the primary (θ^*) angular distribution for the state at 27.2 MeV ($E_{\text{beam}}=80.5$ MeV). In this measurement the detection system was only sensitive to the angular ranges $0 \leq \theta^* \leq 50^\circ$ and $130^\circ \leq \theta^* \leq 180^\circ$. The important feature of the experimental data is that the forward and backward angle yields are of similar intensity. Similar angular distributions were found for the states at 27.9 and 29.0 MeV. For the state at 31.5 MeV there was zero detection efficiency for $\theta^* > 40^\circ$, and consequently no backward angle yield was observed. The angular distribution in Fig. 8 has been calculated by nor-

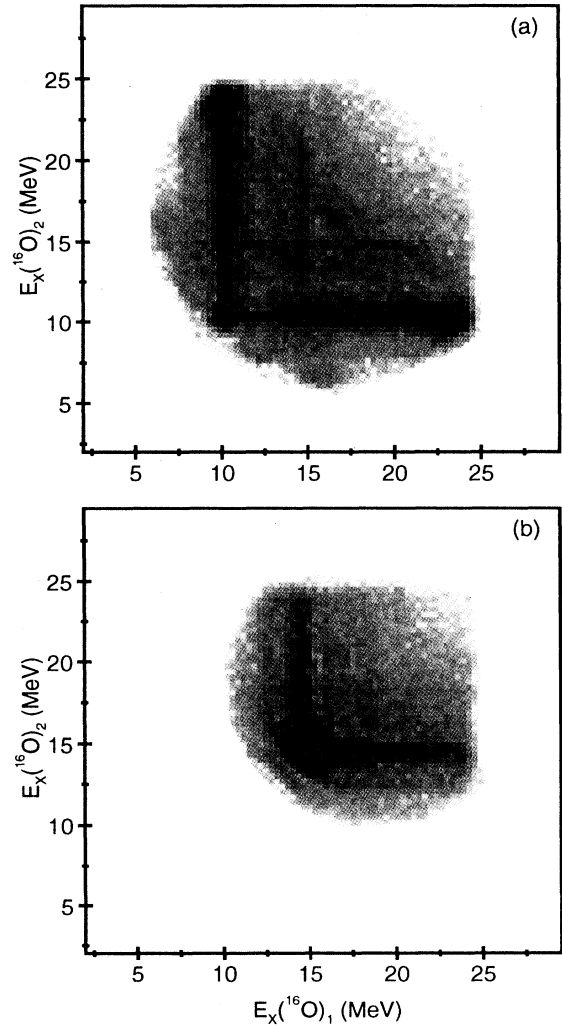


FIG. 5. Plot of the two reconstructed ^{16}O excitation energies for $E_{\text{beam}}=80.5$ MeV, and for final states composed of (a) $^{12}\text{C}(2^+) + ^{12}\text{C} + \alpha$ and (b) $^{12}\text{C}(2^+) + ^{12}\text{C}(2^+) + \alpha$.

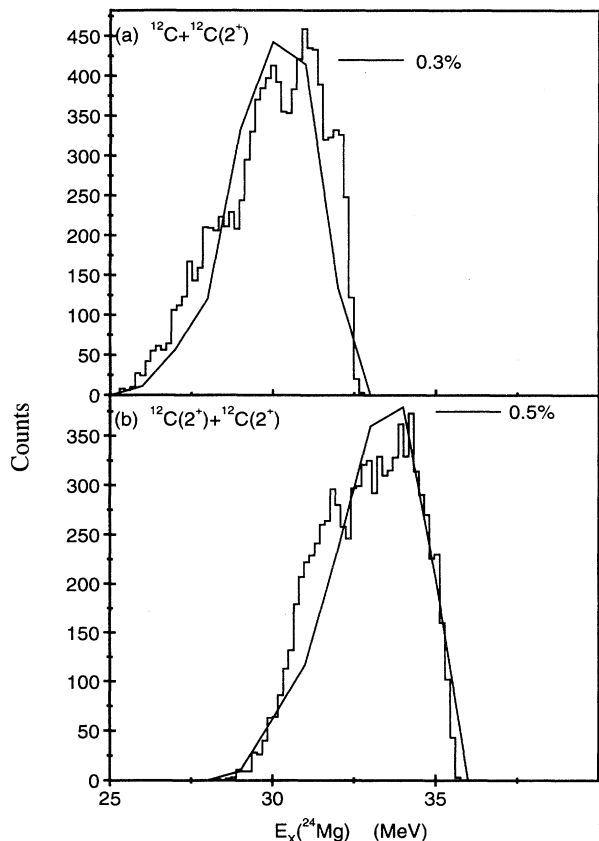


FIG. 6. Reconstructed ^{24}Mg excitation energy spectra for the decay into (a) $^{12}\text{C}(2^+) + ^{12}\text{C}$ and (b) $^{12}\text{C}(2^+) + ^{12}\text{C}(2^+)$. The solid lines are Monte Carlo efficiency calculations.

malizing the data to a Monte Carlo calculation which assumes an isotropic θ^* and a $1/\sin\psi$ angular dependence. The approximate ψ angular distribution and the difficulty of accurately simulating the energy thresholds of the PSSSD's, which are both strip and position dependent, introduce additional uncertainties which are not contained within the error bars in Fig. 8. The energy thresholds are particularly important for the yield in the

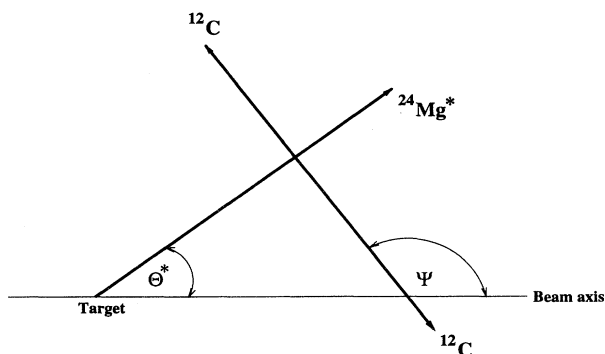


FIG. 7. Illustration of the angles used in the study of the angular distributions. θ^* is the center of mass emission angle of the excited $^{24}\text{Mg}^*$ nucleus, and ψ the subsequent center of mass emission angle of the ^{12}C fragments.

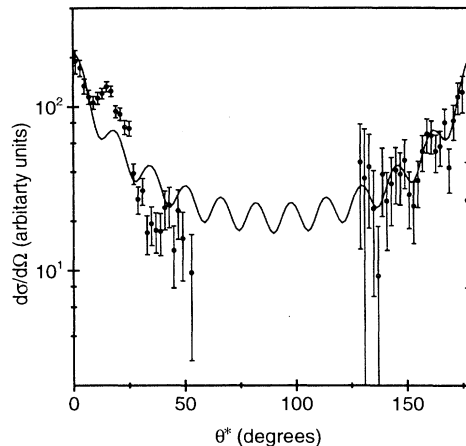


FIG. 8. Angular distribution for the state at 27.2 MeV. The solid line is the result of the calculation described in the text.

angular range $130^\circ \leq \theta^* \leq 180^\circ$ where the dependence on the energy threshold introduces a 35% systematic uncertainty in the normalization at $\theta^* = 175^\circ$, increasing to 80% at $\theta^* = 140^\circ$. The ψ angular approximation in the Monte Carlo calculations may be responsible for some of the structure in the angular distribution.

The experimental angular distribution is compared with the angular distribution predicted by

$$\frac{d\sigma}{d\Omega} = \left| \sum_{l_f} \sum_m \langle l_f - m J m | l_i 0 \rangle Y_{l_f}^m(\theta^*, 0) \right|^2, \quad (3)$$

where l_i and l_f are the initial and final state partial waves, respectively. In this description we have assumed that a single entrance channel partial wave dominates. Figure 8 shows the angular distribution for $l_i = 19\hbar$ and $J = 10\hbar$. The details of the experimental data are clearly not reproduced by the rather simplistic model. However, the calculations are intended to demonstrate the general form of the experimental data if a single angular momentum in the compound ^{28}Si system dominates the reaction cross section. In order to provide a closer description of the experimental data, additional information on the m -substate populations is required, and the Monte Carlo calculations must more accurately reproduce the ψ angular dependence.

Figure 9 shows the forward angle, angular correlations for the states at 27.2, 27.9, 29.0, and 31.5 MeV; these are the only states for which the angular phase space was sufficiently large to observe a well-defined correlation structure. In these four spectra, there appears to be a series of ridges with a central maximum passing through $\theta^* = 0$, $\psi = 90^\circ$.

There are two independent methods for the analysis of these angular correlations. The first of these is a study of the periodicity of the ridge structures. Since the three final state particles are in the ground state with $J=0$, for $\theta^* = 0$ the ^{24}Mg nucleus is aligned in the $m=0$ magnetic substate (taking the quantization axis to be the beam di-

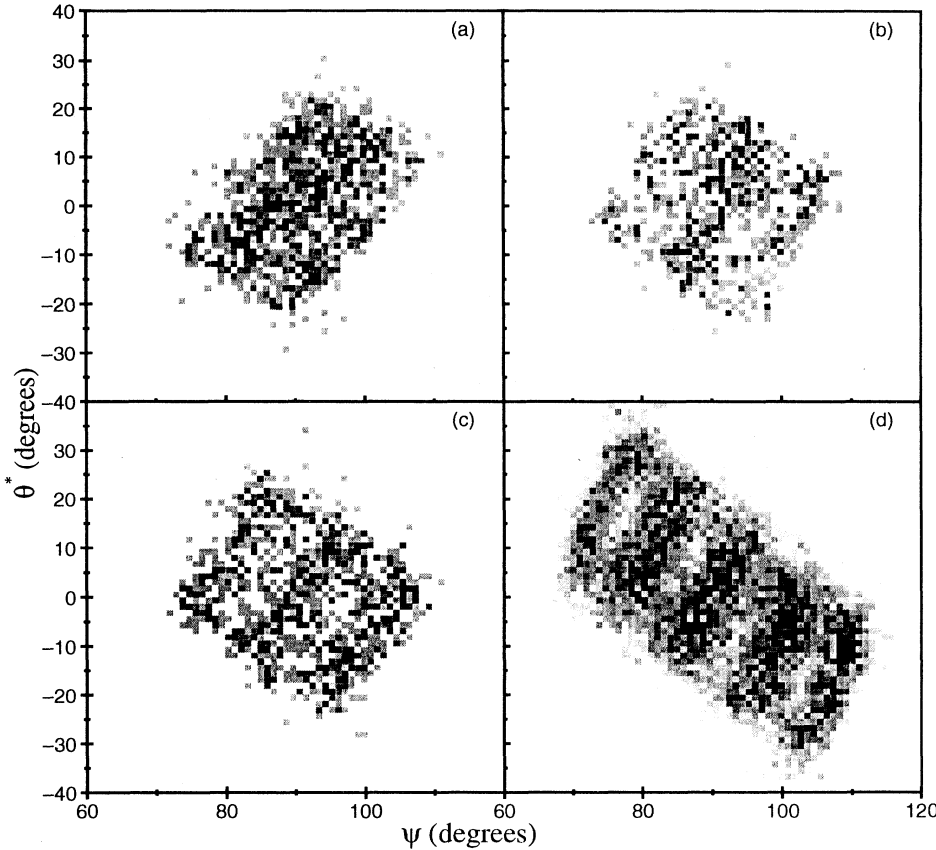


FIG. 9. Angular correlation plots for the states at (a) 27.2 MeV, (b) 27.9 MeV, (c) 29.0 MeV, and (d) 31.5 MeV.

rection). Thus, the decay of the ^{24}Mg nucleus is such that the angular distributions of the two ^{12}C decay products are described by Legendre polynomials of order J , where J is the spin of the ^{24}Mg excited state. At scattering angles away from $\theta^*=0$, the magnetic substate population of the ^{24}Mg nucleus is no longer constrained, and a variety of reaction amplitudes contribute to the angular distributions. Rather than destroying the structure of the correlation pattern which is evident at $\theta^*=0$, the correlation pattern becomes shifted such that

$$\frac{d^2\sigma}{d\theta^*d\psi} \propto |P_J[\cos(\psi + \Delta\psi)]|^2, \quad (4)$$

where $\Delta\psi = \Delta\theta^*l_f/J$ and l_f is the final state grazing angular momentum. Consequently, the θ^* - ψ correlations appear as a series of diagonal ridges which intercept the $\theta^*=0$, ψ axis at points corresponding to the maxima of the function $|P_J(\cos\psi)|^2$. This result was arrived at by Da Silveira [27] by considering the classical relationship between the angular momenta involved in the reaction, and later quantum mechanically by Marsh and Rae [28]. The spin of the ^{24}Mg states can thus be deduced through an examination of the ψ dependence of the correlations along the $\theta^*=0$ axis. However, in this measurement the $\theta^*=0$, ψ coverage is rather restricted. Consequently, we have performed a projection of the correlations onto the $\theta^*=0$ axis at an angle parallel to the ridge structure. This then results in angular distributions whose periodicity,

but not necessarily whose amplitude, reflects the spin of the nucleus, J .

Figure 10 shows the results of these projections for the states at $E_x(^{24}\text{Mg})=27.2, 27.9, 29.0,$ and 31.5 MeV. For the two states at 27.2 and 27.9 MeV these spectra are inconclusive since the ψ angular range is still too restrictive. Further, since the minima in the correlations for these states are rather shallow, this would appear to suggest that there are perhaps a number of states with differing spins contributing to the correlations. For the two states at 29.0 and 31.5 MeV the correlations are much clearer, and indicate spins of $J=12$ and $14\hbar$, respectively.

The second method for determining the spins of the ^{24}Mg states, which is independent of the first, is the study of the gradient of the ridges in the θ^* - ψ correlations, i.e., the angle at which the projections were performed. The gradient of the correlations reflects the angular momenta involved in the reaction, $\Delta\theta^*/\Delta\psi = J/l_f$. If the $^{12}\text{C}(^{16}\text{O}, ^{24}\text{Mg}^*)\alpha$ reaction proceeds through a narrow angular momentum window, then only a few values of l_i (the incident grazing angular momentum) and l_f contribute. Furthermore, if the ^{24}Mg nucleus decays perpendicular to the angular momentum axis \mathbf{J} , then there is a direct relationship between \mathbf{J} and \mathbf{l}_f (i.e., $\mathbf{l}_f = \mathbf{l}_i - \mathbf{J}$) and hence J/l_f is uniquely defined [27,28]. The gradients at which the projections were performed are shown in Table I.

The correlations for the two states at 29.0 MeV ($J = 12\hbar$) and 31.5 MeV ($J=14\hbar$) indicate $l_i=18.8 \pm 0.6\hbar$ and

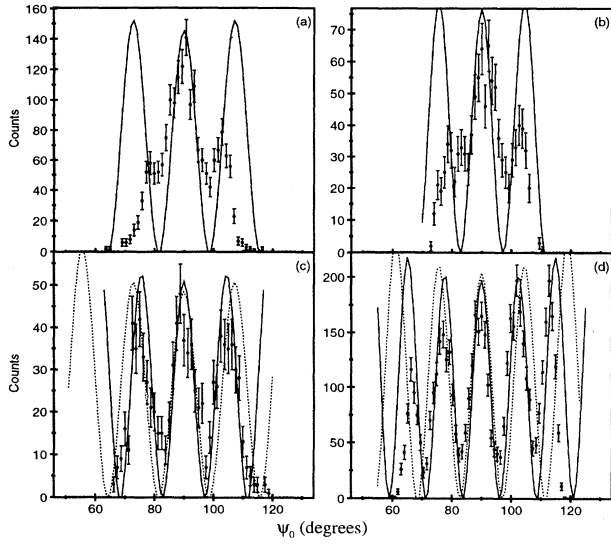


FIG. 10. Angular correlation projections for the $E_{\text{beam}}=80.5$ MeV data, overlaid with Legendre polynomials, for the states at (a) 27.2 MeV with $|P_{10}|^2$, (b) 27.9 MeV with $|P_{12}|^2$, (c) 29.0 MeV with $|P_{12}|^2$ (solid line) and $|P_{10}|^2$ (dotted line), and (d) 31.5 MeV with $|P_{14}|^2$ (solid line) and $|P_{12}|^2$ (dotted line).

$19.5 \pm 0.6\hbar$, respectively. If we then assume $l_i = 19\hbar$, this would imply that for the two states at 27.3 and 28.4 MeV the dominant spins are $J=10$ and $12\hbar$, respectively, (as shown in Fig. 10). However, the angular correlations should be measured over a greater ψ angular range to confirm this interpretation. The uncertainty in the present analysis would suggest a corresponding uncertainty in the deduced spins for these states of $\pm 2\hbar$.

The projected angular correlation for the 27.2 MeV state, measured with the 99 MeV beam energy, is shown in Fig. 11. The periodicity of the correlation is consistent with the $J=10\hbar$ assignment. Furthermore, the projection angle would imply $l_i=21\hbar$ which is consistent with the expected increase in the grazing angular momentum due to the higher beam energy.

With the techniques described above, it is not possible to determine the spins of the states observed in the $^{12}\text{C}(2^+) + ^{12}\text{C}_{\text{gs}}$ and $^{12}\text{C}(2^+) + ^{12}\text{C}(2^+)$ decay channels, since they involve nonspin zero particles.

TABLE I. The values of the entrance channel grazing angular momenta l_i deduced from the gradients of the angular correlations in Fig. 8.

E_x (MeV)	$J(\hbar)$	$\Delta\theta^*/\Delta\psi$	$l_i(\hbar)$
27.2 ^a		1.11 ± 0.08	
27.2 ^b	10	0.90 ± 0.06	21.1 ± 0.9
27.9		1.73 ± 0.08	
29.0	12	1.60 ± 0.13	19.5 ± 0.6
31.5	14	2.90 ± 0.30	18.8 ± 0.6

^a $E_{\text{beam}}=80.5$ MeV.

^b $E_{\text{beam}}=99$ MeV.

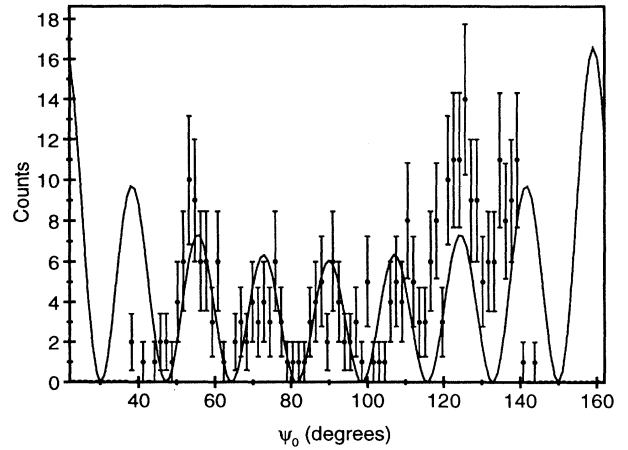


FIG. 11. Angular correlation projection for the 27.2 MeV state ($E_{\text{beam}}=99$ MeV), overlaid with $|P_{10}|^2$.

C. The $^{16}\text{O}(^{16}\text{O}, ^{12}\text{C}^{16}\text{O})\alpha$ reaction

Following the observation of a strong final-state interaction in the $^{12}\text{C}(^{16}\text{O}, ^{12}\text{C}^{16}\text{O})\alpha$ reaction, a search has been performed for evidence for a $^{12}\text{C} + ^{16}\text{O}$ final-state interaction. In this measurement the ^{12}C and ^{16}O nuclei were again detected in the gas-silicon hybrid detectors on opposite sides of the beam axis. However, due to the composition of the target, the majority of the $^{12}\text{C} + ^{16}\text{O}$ coincidences corresponded to inelastic scattering of the ^{16}O beam from the ^{12}C backing. In order to remove this contribution, an analysis of the final state missing momentum was performed, and a requirement that the α recoil energy was >1.5 MeV was imposed. Figure 12 shows the Q -value spectrum for $^{12}\text{C} + ^{16}\text{O}$ coincidences following the application of the recoil energy condition, for the ^{16}O beam energy of 80.5 MeV.

Figure 13 shows a plot of the reconstructed excitation energies of ^{16}O and ^{20}Ne nuclei, assuming two-body

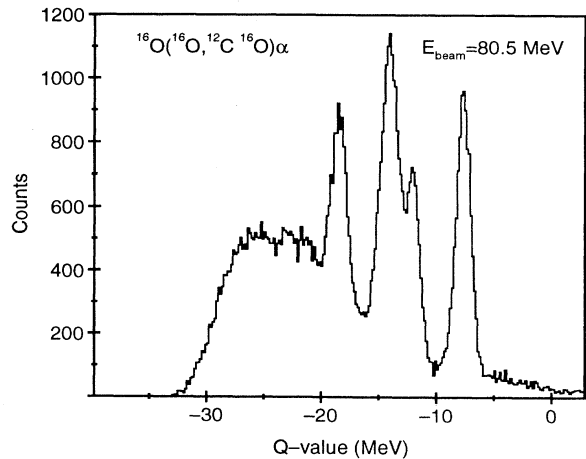


FIG. 12. Three-body Q -value spectrum constructed for the detection of $^{12}\text{C} + ^{16}\text{O}$ and an assumed α recoil.

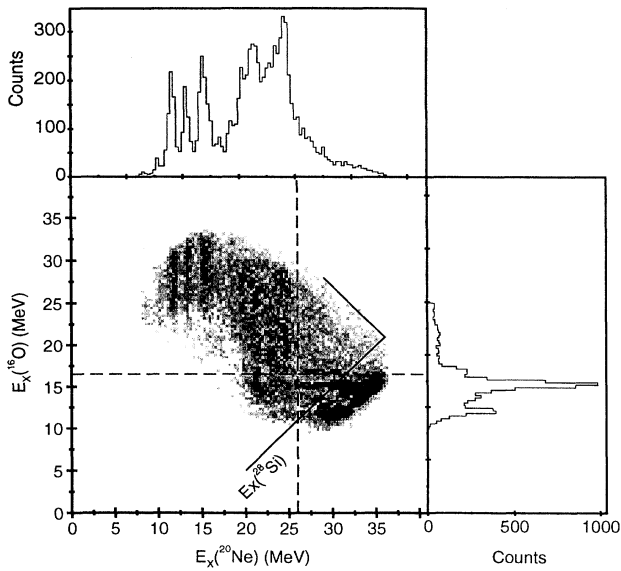


FIG. 13. Plot of the reconstructed ^{16}O and ^{20}Ne excitation energies. The horizontal and vertical loci correspond to ^{16}O and ^{20}Ne excited states, respectively. Evidence for a $^{12}\text{C}\text{-}^{16}\text{O}$ final-state interaction may be observed in the region $E_x(^{16}\text{O}) > 16.5$ MeV and $E_x(^{20}\text{Ne}) > 26$ MeV. The dashed lines represent limits below which data were excluded for the $E_x(^{16}\text{O})$ and $E_x(^{20}\text{Ne})$ projections.

kinematics and that the detected ^{12}C and ^{16}O nuclei are recoil-like particles, corresponding to the reactions $^{16}\text{O}(^{16}\text{O}, ^{16}\text{O}\alpha)^{12}\text{C}$ and $^{16}\text{O}(^{16}\text{O}, ^{12}\text{C}\alpha)^{16}\text{O}$, respectively. This spectrum corresponds to the condition that all of the final state particles are in the ground state. There is clear evidence for the $^{12}\text{C}+^{16}\text{O}+\alpha$ final state being produced through the α decay of excited states in ^{16}O and ^{20}Ne , which correspond to horizontal and vertical loci, respectively. In the ^{16}O case, the decay proceeds from excited states at 11.2 and 14.8 MeV, and the alpha decay of the ^{20}Ne nucleus is predominantly from states between 10 and 25 MeV [$E_x(^{20}\text{Ne})=11.9, 13.5, 15.3, 21.1,$ and 24.2 MeV] which can be associated with states observed in the $^{12}\text{C}(^{16}\text{O}, ^{20}\text{Ne}^*)^8\text{Be}$ reaction [29]. There is only a weak indication of evidence for diagonal ridges in this spectrum in the region $E_x(^{16}\text{O}) > 16.5$ MeV and $E_x(^{20}\text{Ne}) > 26$ MeV. The data appearing in this energy window are shown projected onto the ^{28}Si excitation energy axis in Fig. 14. There would appear to be possibly some evidence for states at 27.3, 28.1, and 28.6 MeV. The statistics and the angular correlations for these states were too restricted to yield angular momentum information, consequently we are unable to suggest spins.

An examination of the relative yields for the two reactions $^{12}\text{C}(^{16}\text{O}, ^{12}\text{C}^{12}\text{C})\alpha$ and $^{16}\text{O}(^{16}\text{O}, ^{16}\text{O}^{12}\text{C})\alpha$ would indicate that the reaction cross section for the second reaction is a factor of 5 smaller than the first. This is based upon the assumption that the angular distributions are similar in both cases. The more restrictive energy cuts imposed in the analysis of the $^{12}\text{C}+^{16}\text{O}$ data and the use of symmetric detector angles with an asymmetric decay

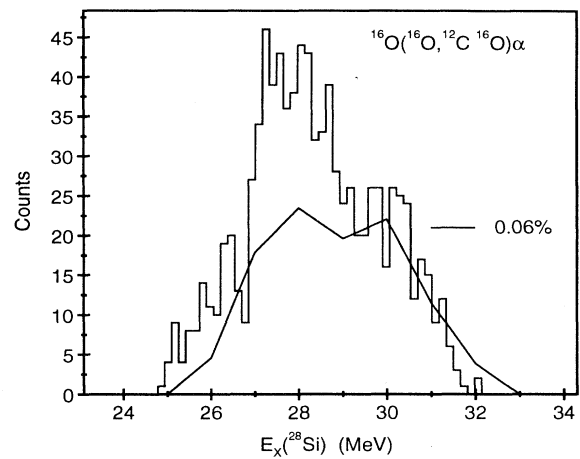


FIG. 14. ^{28}Si excitation energy spectra overlaid with the calculated detection efficiency.

channel, results in nearly an order of magnitude reduction in the detection efficiency for the fission of ^{28}Si when compared to ^{24}Mg . These contributions and the difference in the ^{12}C and ^{16}O target thickness accounts for the factor of 10 difference in the observed yields.

No evidence for any $^{12}\text{C}+^{16}\text{O}$ breakup yield was observed for the beam energy of 99 MeV, even though the detectors were sensitive to a similar ^{28}Si excitation energy region.

IV. DISCUSSION

The results of the measurements for the breakup of ^{24}Mg into two ^{12}C nuclei, populated in the $^{12}\text{C}(^{16}\text{O}, ^{24}\text{Mg}^*)\alpha$ reaction are summarized in Table II. We have observed a number of excited states in the region 23 to 32 MeV, with spins from 10 to $14\hbar$.

Costanzo *et al.* [19] reported a spin of $J = 12 \pm 2\hbar$ for a state at 30.7 MeV, which we have associated with the state at 31.5 MeV in the present measurement for which we assign a spin of $14\hbar$. The uncertainty in this earlier measurement was due to the restricted $\theta^*\text{-}\psi$ angular coverage which made the interpretation of the angular correlations difficult. We have confirmed that if the data

TABLE II. A summary of the states observed in this measurement of the $^{12}\text{C}(^{16}\text{O}, ^{12}\text{C}^{12}\text{C})\alpha$ reaction.

E_x (MeV)	$J(\hbar)$
(23.0)	
25.4	
26.2	
27.2	(10)
27.9	(12)
29.0	12
(29.7)	
31.5	14
(32.6)	

in the present measurement are similarly restricted it is possible to misinterpret the spin of the state as $J = 12\hbar$. Costanzo *et al.* [20] have also proposed $J=14$ assignments for the states at 35.1 and 36.5 MeV. The angular distribution measurements for these states were limited to the observation of only three maxima, centered around $\psi=90^\circ$, hence it would appear to be difficult from this evidence alone to confidently distinguish between $J=14$ and $J=16$. However, the gradient of the correlations, Fig. 4 in Ref. [20], indicate that $l_i=22.5$ and $25.5\hbar$ for $J=14$ and 16, respectively. The systematics of the measurements performed at 80.5 and 99 MeV would suggest that $l_i=23\hbar$ for $E_{\text{beam}}=113$ MeV. This would appear to support the $J=14$ assignment. However, this should be confirmed by measuring the angular distributions over a wider ψ range.

Figure 15 shows a comparison of the measured energies and spins of the states observed in the $^{12}\text{C}(^{16}\text{O}, ^{12}\text{C}^{12}\text{C})\alpha$ reaction with the energy-spin systematics of the barrier resonances. The three states at 27.9, 29.0, and 31.5 MeV appear to lie outside the locus of the barrier resonances, whereas the states at 27.2, 35.1, and 36.5 MeV appear to correlate with the trend of the barrier resonances. These measurements thus indicate that these ^{24}Mg states may not all be related to the barrier resonances, and that perhaps a combination of ^{24}Mg configurations may be required to fully explain the data. Indeed, if the states at 35.1 and 36.5 MeV were 16^+ , it might be conjectured that a separate band is involved.

The symmetry of the primary (θ^*) angular distributions about $\theta^*=90^\circ$, which has been observed for the states at 27.2, 27.9, and 29.0 MeV states, is consistent with an excitation process which is linked to the ^{28}Si compound nucleus. Earlier measurements had suggested that a transfer-type process may be responsible for the excitation of the ^{24}Mg states. Costanzo *et al.* [20] had

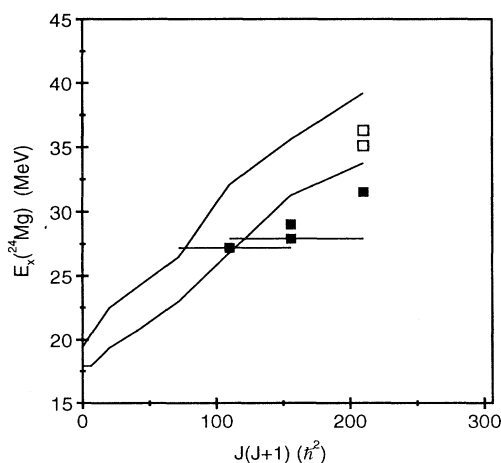


FIG. 15. The energy-spin systematics of resonances observed in the $^{12}\text{C}\text{-}^{12}\text{C}$ interaction. The solid lines represent the highest and lowest energy resonances observed in the $^{12}\text{C}(^{12}\text{C},\alpha)$ and $^{12}\text{C}(^{12}\text{C},^8\text{Be})$ reactions [1,22,21]. The filled squares are the states for which spins could be determined in the present measurement, and the open squares are the data of Costanzo *et al.* [20].

found that the Brink matching conditions [30] could describe both the excitation energy and spins of the observed states, and thus concluded that either (i) a transfer of a ^{12}C from the ^{16}O projectile to the ^{12}C target, or (ii) a transfer of ^8Be from the ^{12}C target to the ^{16}O beam, were responsible for the excitation process. The observation of a θ^* angular distribution which is forward and backward peaked with similar intensity would suggest that direct transfer may not be the excitation process. For the transfer reaction to reproduce the experimental θ^* angular distribution, the ^8Be and ^{12}C transfer cross sections must be of equal magnitude, i.e., the spectroscopic factors for the transfer of ^8Be and ^{12}C nuclei from ^{12}C and ^{16}O , respectively, are the same. This description would further require that two different transfer processes lead to the population of the same states.

Furthermore, from the Brink matching conditions, an increase in the beam energy would be expected to result in an increased angular momentum transfer. Contrary to this, this experiment has observed that when the beam energy was increased from 80.5 to 99 MeV it was the lowest spin state ($J=10$) which was favored over those of higher spins ($J=12, 14$). Again, this would seem to point to the role of the $^{28}\text{Si}^*$ compound system in the reaction process, and/or perhaps the rather different nature of the 27.2 MeV state. This latter feature may indicate that different structures are being populated in the ^{28}Si nucleus at the two energies, which preferentially couple, through the α -decay process, to particular states in ^{24}Mg which possess a close structural link to those in ^{28}Si .

V. SUMMARY AND CONCLUSIONS

The $^{12}\text{C}(^{16}\text{O}, ^{24}\text{Mg}^* \rightarrow ^{12}\text{C} + ^{12}\text{C})\alpha$ and the $^{16}\text{O}(^{16}\text{O}, ^{28}\text{Si}^* \rightarrow ^{12}\text{C} + ^{16}\text{O})\alpha$ reactions, studied with $E_{\text{beam}}=80.5$ MeV, appear to populate states in ^{24}Mg and ^{28}Si in the excitation energy intervals 23 to 33 MeV and 26 to 30 MeV, respectively. In the case of ^{24}Mg , we have made spin measurements for several of the observed states. The deduced energy-spin systematics would appear to place several of the states below the locus of the barrier resonances. These data and the earlier measurements of Costanzo *et al.* indicate that the ^{24}Mg states may be associated with a combination of nuclear configurations which may include that connected with the barrier resonances. The angular distributions and energy dependence of the reaction cross section further suggest that the excitation mechanism for the population of these states may be closely linked to the ^{28}Si compound nucleus.

ACKNOWLEDGMENTS

The authors would like to acknowledge the assistance of ANU personnel in running the accelerator, in particular R.G. Cresswell. M.F. would like to thank the Engineering and Physical Sciences Research Council for financial support.

- [1] K.A. Erb and D.A. Bromley, in *Treatise on Heavy-Ion Science*, edited by D.A. Bromley (Plenum, New York, 1985), Vol. 3.
- [2] J. Wilczynsky, K. Siwek-Wilczynska, Y. Chan, E. Chavez, S.B. Gazes, and R.G. Stokstad, *Phys. Lett. B* **181**, 229 (1986).
- [3] B.R. Fulton, S.J. Bennett, C.A. Ogilvie, J.S. Lilley, D.W. Banes, W.D.M. Rae, S.C. Allcock, R.R. Betts, and A.E. Smith, *Phys. Lett. B* **181**, 233 (1986).
- [4] A.J. Lazzarini, E.R. Cosman, A. Sperduto, S.G. Steadman, W. Thomas, and G.R. Young, *Phys. Rev. Lett.* **40**, 1426 (1978).
- [5] K. Nagatani, T. Shimoda, D. Tanner, R. Tribble, and T. Yamaya, *Phys. Rev. Lett.* **40**, 1480 (1979).
- [6] M. Ichimura, E. Takada, T. Yamaya, and K. Nagatani, *Phys. Lett.* **101B**, 31 (1981).
- [7] N. Takahashi, T. Yamaya, R.E. Tribble, E. Takada, Y.W. Lui, D.M. Tanner and K. Nagatani, *Phys. Lett.* **108B**, 177 (1982).
- [8] T.M. Cormier, J. Applegate, G.M. Berkowitz, P. Braun-Munzinger, P.M. Cormier, J.W. Harris, C.M. Jachcinski, and L.L. Lee, Jr., *Phys. Rev. Lett.* **38**, 940 (1977).
- [9] W.D.M. Rae, R.G. Stokstad, B.G. Harvey, A. Dacal, R. Legrain, J. Mahoney, M.J. Murphy, and T.J.M. Symons, *Phys. Rev. Lett.* **45**, 884 (1980).
- [10] W.D.M. Rae, *Phys. Lett.* **105B**, 417 (1981).
- [11] T. Shimoda, S. Simoura, T. Fukuda, M. Tanaka, H. Ogata, I. Miura, E. Takada, M.K. Tanaka, K. Takimoto, and K. Katori, *J. Phys. G* **9**, L199 (1983).
- [12] T. Murakami, E. Ungricht, N. Takahashi, Y.E. Lui, Y. Mihara, R.E. Neese, E. Takada, D.M. Tanner, R.E. Tribble, and K. Nagatani, *Phys. Rev. C* **29**, 847 (1984).
- [13] W.D.M. Rae, A.J. Cole, B.G. Harvey, and R.G. Stokstad, *Phys. Rev. C* **30**, 158 (1984).
- [14] A. Szanto de Toledo, M.M. Coimbra, N. Carlin Filho, T.M. Cormier, and P.M. Stwertka, *Phys. Rev. Lett.* **47**, 632 (1981).
- [15] P. Stwertka, T.M. Cormier, M. Herman, N. Nicholas, A. Szanto de Toledo, M.M. Coimbra, and N. Carlin Filho, *Phys. Rev. Lett.* **49**, 640 (1982).
- [16] A.J. Lazzarini, S.G. Steadman, R. Ledoux, A. Sperduto, G.R. Young, K. Van Bibber, and E.R. Cosman, *Phys. Rev. C* **27**, 1550 (1983).
- [17] J.S. Karp, D. Abriola, R. L. McGrath, and W.A. Watson III, *Phys. Rev. C* **27**, 2649 (1983).
- [18] E. Costanzo, M. Lattuada, S. Romano, D. Vinciguerra, M. Zadro, N. Cindro, M. Freer, B.R. Fulton, and W.D.M. Rae, *Europhys. Lett.* **14**, 221 (1991).
- [19] E. Costanzo, M. Lattuada, S. Romano, D. Vinciguerra, M. Zadro, N. Cindro, M. Freer, B.R. Fulton, and W.D.M. Rae, *Phys. Rev. C* **44**, 111 (1991).
- [20] E. Costanzo, M. Lattuada, S. Pirrone, S. Romano, D. Vinciguerra, and M. Zadro, *Phys. Rev. C* **49**, 985 (1994).
- [21] N. Cindro, *Rev. Nuovo Cimento* **4** (no. 6), 1 (1981).
- [22] N.R. Fletcher, J.D. Fox, G.J. Kekelis, G.R. Morgan, and G.A. Norton, *Phys. Rev. C* **13**, 1173 (1976).
- [23] K.A. Erb and D.A. Bromley, *Phys. Rev. C* **23**, 23 (1981).
- [24] N. Curtis *et al.*, *Nucl. Instrum. Methods Phys. Res. Sect. A* **351**, 359 (1994).
- [25] F. Ajzenberg-Selove, *Nucl. Phys.* **A460**, 1 (1986).
- [26] W.D.M. Rae and R.K. Bhowmik, *Nucl. Phys.* **A420**, 320 (1984).
- [27] E.F. Da Silveira, *Proceedings of the 14th winter Meeting on Nuclear Physics, Bormio, 1976* (unpublished).
- [28] S. Marsh and W.D.M. Rae, *Phys. Lett.* **153B**, 21 (1985).
- [29] W.D.M. Rae, S.C. Allcock, and J. Zhang, *Nucl. Phys.* **A568**, 286 (1994).
- [30] D.M. Brink, *Phys. Lett.* **40B**, 37 (1972).

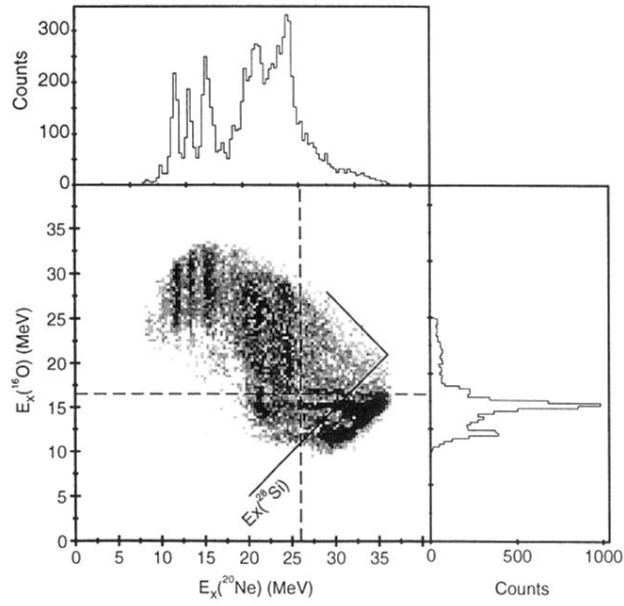


FIG. 13. Plot of the reconstructed ^{16}O and ^{20}Ne excitation energies. The horizontal and vertical loci correspond to ^{16}O and ^{20}Ne excited states, respectively. Evidence for a $^{12}\text{C}\text{-}^{16}\text{O}$ final-state interaction may be observed in the region $E_x(^{16}\text{O}) > 16.5$ MeV and $E_x(^{20}\text{Ne}) > 26$ MeV. The dashed lines represent limits below which data were excluded for the $E_x(^{16}\text{O})$ and $E_x(^{20}\text{Ne})$ projections.

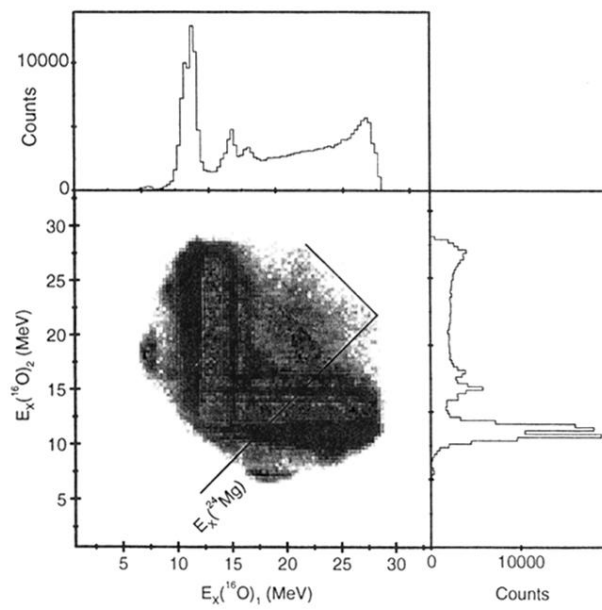


FIG. 2. Plot of the two reconstructed ^{16}O excitation energies. The horizontal and vertical loci correspond to ^{16}O excited states. Evidence for a ^{12}C - ^{12}C final-state interaction may be observed in the region $E_x(^{16}\text{O})_1 > 15$ MeV and $E_x(^{16}\text{O})_2 > 15$ MeV.

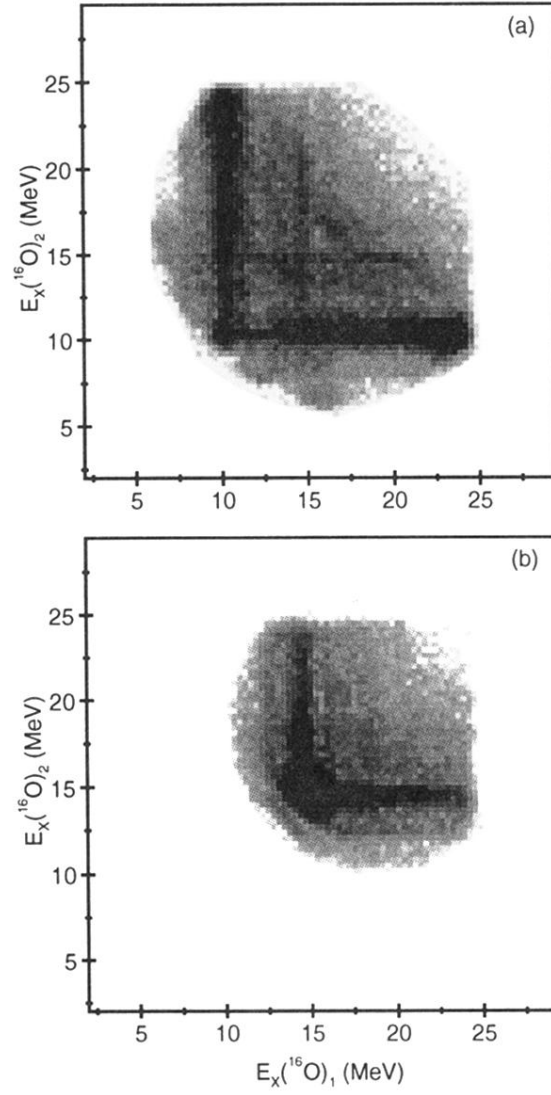


FIG. 5. Plot of the two reconstructed ^{16}O excitation energies for $E_{\text{beam}}=80.5$ MeV, and for final states composed of (a) $^{12}\text{C}(2^+) + ^{12}\text{C} + \alpha$ and (b) $^{12}\text{C}(2^+) + ^{12}\text{C}(2^+) + \alpha$.

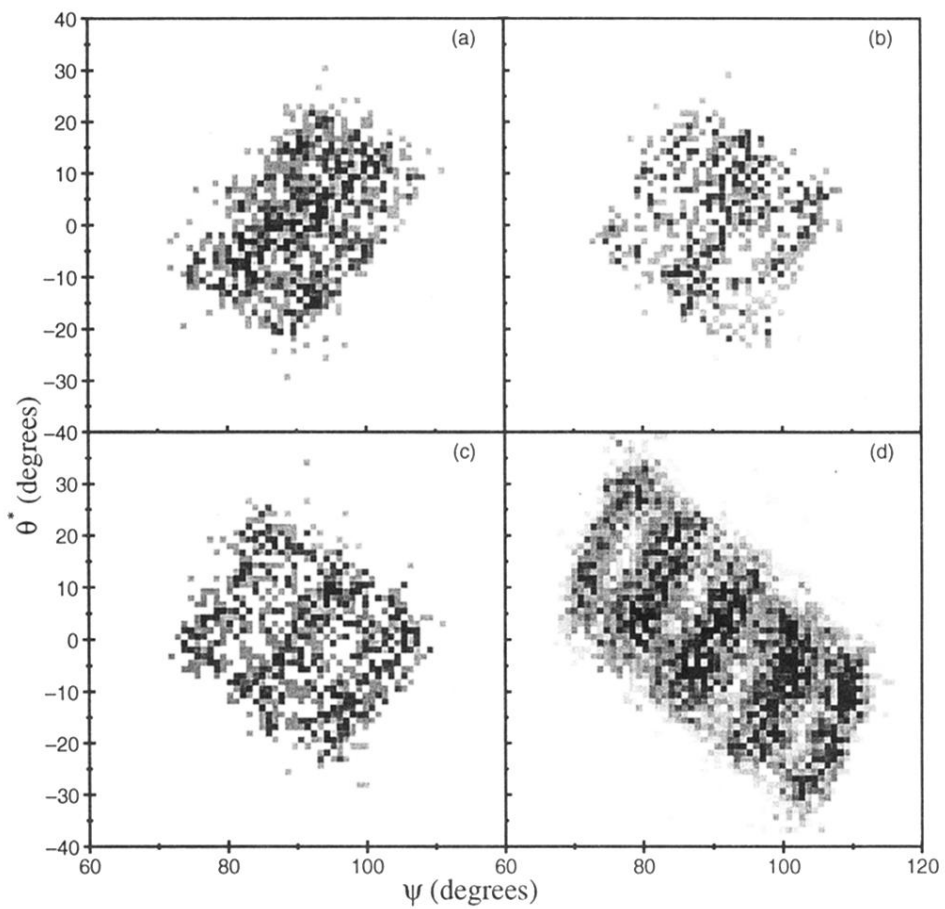


FIG. 9. Angular correlation plots for the states at (a) 27.2 MeV, (b) 27.9 MeV, (c) 29.0 MeV, and (d) 31.5 MeV.